DIMENSIONALITY REDUCTION FOR IMPROVED SOURCE SEPARATION IN FMRI DATA

Rudolph L. Mappus IV, David Minnen and Charles Lee Isbell Jr.
College of Computing, Georgia Tech, 85 Fifth St. NW, Atlanta, USA

Keywords: Dimensionality reduction, ICA, fMRI.

Abstract: Functional magnetic resonance imaging (fMRI) captures brain activity by measuring the hemodynamic response. It is often used to associate specific brain activity with specific behavior or tasks. The analysis of fMRI scans seeks to recover this association by differentiating between task and non-task related activation and by spatially isolating brain activity. In this paper, we frame the association problem as a convolution of activation patterns. We project fMRI scans into a low dimensional space using manifold learning techniques. In this subspace, we transform the time course of each projected fMRI volume into the frequency domain. We use independent component analysis to discover task related activations. The combination of these methods discovers sources that show stronger correlation with the activation reference function than previous methods.

1 INTRODUCTION

Functional magnetic resonance imaging (fMRI) captures neural activation patterns by measuring the hemodynamic response in cranial tissue through sampling discrete regions of the brain, referred to as voxels (Dogil et al., 2002). Each voxel represents the aggregate hemodynamic response of a region of neurons. Behavioral experiments using fMRI are designed to evoke activation in a hypothesized *region of interest* (ROI) in the brain. The ROI represents an anatomical region of the brain believed to be where functional processing of a specific behavioral task occurs. Experimental trials in these designs use a behavioral task meant to evoke activation in the ROI. Control trials do not evoke ROI activation.

Unfortunately, locating significant differences between active and non-active voxels is challenging because of the inherent latencies and artifacts in fMRI signal acquisition (Josephs et al., 1997). Furthermore, the hemodynamic activation level of neighboring voxels influences voxel activation, producing less accurate spatial activation maps.

Traditional analysis methods such as statistical parametric mapping (SPM) use statistical tests to demonstrate significant differences between the time course activation of particular voxels in the control and experimental tasks (Friston, 2003). By contrast, the objective of component analysis methods—such as independent components analysis (ICA)—is to recover components whose time course activation correlates with the task-based reference function: $\text{argmax}_{a\in\{A\}}\,\rho(r,a)$, where r is the reference activation time course that represents the ideal activation during the trial, and a is the component activation time course.

Although ICA has been shown to work for simple block experimental designs, it has some limitations. In particular, ICA has been used successfully when combined with *a priori* anatomical information about activation areas (McKeown et al., 1998). Furthermore, simple ICA does not account for the delayed composition effects that can arise in fMRI analysis.

The contribution of this work is to frame the problem of the combined latencies of the hemodynamic response and the signal acquisition process as a convolution of the hemodynamic response functions of spatially independent components. Framed this way, we can address these confounding spatial and temporal influences, by first using nonlinear manifold learning to constrain source separation and to remove voxels that do not help distinguish between task and non-task activation. We generate a frequency space representation of the reduced features for convolutive source separation using ICA. Our method allows us to handle delayed composition effects and to select ROIs

L. Mappus IV R., Minnen D. and Lee Isbell Jr. C. (2008).
DIMENSIONALITY REDUCTION FOR IMPROVED SOURCE SEPARATION IN FMRI DATA.
In *Proceedings of the First International Conference on Bio-inspired Systems and Signal Processing*, pages 308-313
DOI: 10.5220/0001068403080313

without specific a priori anatomical knowledge of the ROI. Thus, we are able to limit type II errors.

2 PREVIOUS WORK

Independent Components Analysis. Time domain independent component analysis (ICA) works on discrete time, linear dynamical systems where a latent process generates a set of observables (McKeown et al., 1998). A *k*-vector of random variables represents the state of the process at each time step. In such a system, latent variables are linearly mixed to give rise to the observable variables at each time step. First-order Markov dynamics govern state transitions within the process defined by a $k \times k$ matrix M (Roweis and Ghahramani, 1999).

Formally, $X = AS$, where X is a $k \times t$ *observation matrix*, A is a *mixing matrix* and S is the $k \times t$ matrix representing the time course evolution of the latent random variables. ICA recovers an *unmixing matrix* A^{-1} for the observation matrix X. A^{-1} produces a set of statistically independent components from the data. Under certain assumptions, the components represent the (possibly scaled) evolution of the original latent process. In this case, the mixing matrix A represents the degree to which a component participates in the generation of the observation data at each time step. For the analysis of fMRI scans, we assume that the separation problem in the reduced dimension problem is determined, which means that the number of sources is equal to the number of sensors (voxels). In the determined case, the discovered independent components can be interpreted as underlying *causes* of observations, especially when one believes that: (1) observed features are generated by the interaction of a set of independent hidden random variables, and (2) these hidden variables are likely to be kurtotic (*i.e.* discriminative and sparse). These assumptions are reasonable for fMRI analysis because of existing neurological evidence for functional modularity in the brain and the specific requirements of the experimental task.

Time domain applications of ICA assume an instantaneous linear mixture model at each time step. McKeown *et al.* (McKeown et al., 1998) applied ICA to fMRI data from a simple block-design experiment and found correlated activation signal for a component corresponding to the region of interest (McKeown et al., 1998).

Manifold Learning and fMRI. Manifold learning has been applied to fMRI time domain data directly (Shen and Meyer, 2006). In this case, the intrinsic dimensionality represents spatially independent voxel activations and the objective is to generate clusters matching ground truth classification. The intuition is that task related activated voxels will cluster together in the representation. The interpretation of the manifold is that it captures information about the geometry of the volume space. A key issue with direct application is that target signals in a behavioral study are often not the high ranking elements generated using principle components analysis (PCA) and ICA (McKeown et al., 1998). These less significant activations typically rank in the latter component quartiles.

Convolutional Blind Source Separation. Blind separation of convolutional sources has applications in a number of signal processing domains, including fMRI (Pederson et al., 2007; Anemuller et al., 2003). Here, we assume a linear convolution of sources in the time domain and model observations at time t as:

$$x(t) = \sum_{k=0}^{K-1} A_k s(t-k) + v(t) \quad (1)$$

where K is the finite impulse response (FIR) length. In frequency space, source separation is performed for each frequency. For the purpose of analyzing fMRI data, where there is a relatively limited temporal extent, we choose a window function that minimizes band overlap.

$$\mathbf{W}(\omega) = \mathbf{A}(\omega)\mathbf{S}(\omega) + \mathbf{V}(\omega) \quad (2)$$

3 COMBINED APPROACH

Our approach to fMRI analysis seeks to combine the strengths of manifold learning, convolution in frequency space, and complex ICA in order to improve the accuracy of recovered brain activity components.

Manifold learning has not been applied to time domain data as preprocessing for component analysis. Furthermore, manifold learning techniques reduce the dimensionality of the ROI, making component analysis more effective at source separation. In fact, much of the ROI is not significantly activated and correlated to the reference function. We want to reduce the dimensionality of these voxels before source separation.

Using ICA in the frequency domain allows us to treat convolution of components as a product, which in turn allows a computationally feasible algorithm to solve the convolutive blind source separation problem. Using this version of the source separation problem is important because voxels near each other in the brain may exhibit delayed influences during recording. Using a convolutive model instead of an instantaneous mixing model provides the ability to capture this influence and properly separate the components.

3.1 Manifold Learning

Before transformation into the frequency domain and subsequent component analysis, we apply a manifold learning algorithm to reduce the size of the voxel set. The dimensionality reduction serves two purposes. First, it reduces the computational burden of the relatively expensive ICA computation. More importantly, manifold learning allows researchers to include a large ROI in order to avoid Type II errors caused by failing to include a relevant voxel in the analysis. The dimensionality reduction algorithm can then reduce the region based on the observed activation levels, thereby achieving a manageable size while minimizing the risk of excluding relevant voxels.

We experiment with several different manifold learning methods: local linear embedding (LLE) (Roweis and Saul, 2000), isomap (Tenenbaum et al., 2000), Laplacian eigenmaps (Belkin and Niyogi, 2003) and diffusion maps (Coifman and Lafon, 2006). Diffusion maps were used in previous work with fMRI (Shen and Meyer, 2006), while LLE and isomap are both standard methods for manifold learning and provide a basis for comparison.

3.2 Complex ICA

In order to convert the time course of voxel activations into the frequency domain, we use the short–time Fourier transform (STFT) with a window size adapted for each dataset. In the case of the left/right dataset (described in detail in the following section), the window size equals the ratio of the hemodynamic response latency to volume acquisition latency. Each STFT generates frequency vectors for a specific temporal window, which are grouped into frequency vectors and analyzed via complex ICA. The Fourier transforms represent signals in each bin in the frequency domain as complex values. We apply complex-fastICA (Bingham and Hyvarinen, 2000) to each bin, so that the generated components are frequency specific.

3.3 Component Comparison

We select components with activation sharing high correlation to the reference activation function. We consider these components to be task related. In the time domain, application of ICA generates the activation of independent sources in the columns of the unmixing matrix A, and correlation of these columns to the reference function indicates task relatedness. In the frequency domain, where there STFT generates a set of frequency bins, the objective is to find components in each frequency bin that are task related. We generate the reference activation function using the same parameters (same spectral extent, same bin parameters) used to generate the STFT for the observation set. We use the standard distance measure for complex vectors: $\sum_i |x|^2$. For each bin, we find the highest correlated activation course: $\text{argmax}_a \rho(a,r)$.

4 EXPERIMENTS

Here, we present results of experiments comparing performance of the manifold learning techniques and complex source separation alone. The datasets are meant to demonstrate method performance in a simple, controlled task as well as actual study data.

4.1 Left/right Motor Task

To evaluate our method, we begin with a simple example: consider an fMRI scan sequence of a single subject performing a repetitive right- or left-hand finger movement task (Hurd, 2000). The objective is to find task related activated components of hand movements in the ROI. For the ROI, we selected a window of voxels in a region based on correlation values to the reference function using time domain ICA. In the motor task, 80 volumes were sampled at a constant rate for each task: left-hand/right-hand finger move. We defined a ROI in slices 13,14,15,16, loosely defined around the temporal area of the motor cortex. Scans of left hand tasks are concatenated to scans of right hand tasks, 160 scans total. Given this organization, the reference activation function for left hand tasks is defined as a delta function: $\delta(x \geq 80)$.

First, we want to test how manifold learning techniques assist in time domain separation. In this case, we compare the correlation of component activations recovered by ICA to reference function activation. We compare the best correlation values generated using ICA alone as well as with the various manifold learning techniques. These are all performed using the time domain data (see Table 1). The manifold learning methods do not recover correlated activation of components as well as using ICA alone in this case.

For the STFT, we use a parameterization for each dataset. In the case of the left/right dataset, the window size is the ratio of the hemodynamic response latency to volume acquisition latency. We consider the measured values of voxels v_i through time $t_{i\in\{1\ldots\tau\}}$. Each STFT generates frequency vectors for each window. We group frequency vectors from each STFT and apply component analysis to the resulting matrices. Computing the inverse transform of the compo-

Table 1: Comparison of correlation values to reference function using manifold learning in time domain.

Method	Max ρ	p-value
Diff Map	0.1407	0.1
Isomap	0.3470	0.001
LLE	0.2052	0.01
LE	0.2236	0.005
ICA	0.7395	0.0001

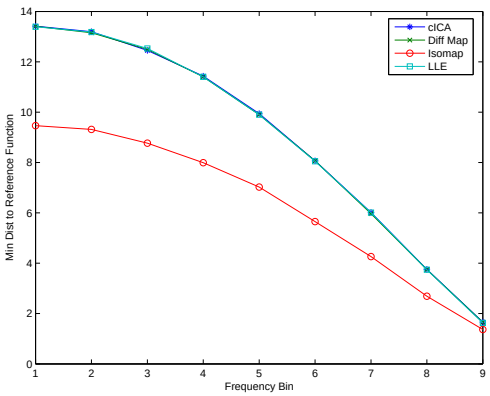

Figure 1: Comparison of minimum distances to reference function between manifold learning method preprocessing and complex ICA. Minimum distance for each method in each STFT frequency bin.

nent produces a time domain representation of the signal. However, due to the window overlap in the STFT, this time scale is not appropriate for comparison in the original observation space.

We compare the performance in the left/right task between the various manifold learning algorithms and complex ICA in the frequency domain without manifold learning (see Table 1). To compare methods, we use the minimum distance of component activation to reference function activation in each frequency bin. In this case, manifold learning using diffusion maps and local linear embedding perform slightly better than complex ICA alone.

4.2 Postle *et Al.* Study

Postle *et al.* (Postle et al., 2000) measured activation of five participants in four behavioral tasks: forward memory, manipulate memory, guided saccade, and a free saccade task. Subjects completed 96 trials: 8 blocks of 12 trials each. Within each block, subjects received an equal number of task trials, in random order. Subjects were presented with a static arrangement of squares on a screen. Signals were acquired using a GE 1.5T scanner with 3.75mm^2 in-plane resolution and 5mm inter-slice distance. Volumes were 21 slices, and volume acquisition time was 2s; 17 volumes were acquired per trial. Inter-trial time was 7s. By comparing voxel activation values in each experimental task in the ROI, Postle *et al.* showed no significant difference in voxel activations between control and experimental tasks.

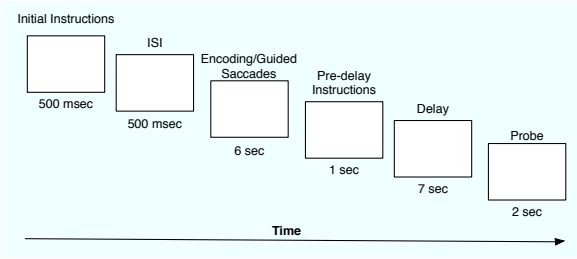

Figure 2: Trial event sequence (Postle et al., 2000). Initial instructions indicate what the memory task will be. After ISI, a sequence of highlighted boxes (see Figure 3) or fixation points appear. Pre-delay instructions indicate whether the memory task is "forward," "down to up," or "fixate." After the delay, the probe is shown.

Figure 2 shows the trial sequence. First, subjects are told what the trial task will be: "memory," "no memory," or "free eye movements." Following an interstimulus interval (ISI) of 500ms, subjects receive the sequence of highlighted squares (Figure 3) followed by further instructions: "forward," "down-to-up," or "fixate." After the return to baseline delay, subjects receive the probe: a highlighted square in the sequence.

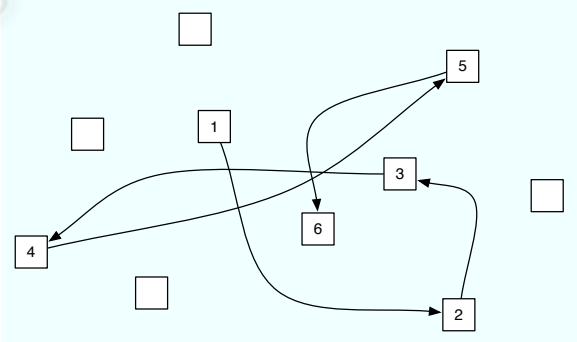

Figure 3: Memory task stimulus. A fixed number of squares are oriented on a screen. During memory tasks, a sequence of the squares are highlighted in a random order. An example highlight sequence for memory is shown.

Behavioral Tasks. During forward memory, manipulate memory, and guided saccade tasks, a sequence of squares was highlighted followed by a delay and then a task prompt (see Figures 2&3). In forward memory tasks, subjects were presented a sequence of highlighted squares. Then, given one of highlighted

Table 3: Comparison of minimum distances to reference function activation between manifold learning methods in combination with complex ICA and complex ICA alone. For each bin (columns), the minimum distance for each method is shown (*i.e.* the distance of the best matching components in each frequency bin).

	1	2	3	4	5	6	7	8	9
Subject H									
ICA	30.9077	29.5631	28.0292	25.5206	22.1484	18.0443	13.3546	8.1448	2.8922
Isomap	29.9395	29.4552	27.8957	25.4514	22.1252	18.0155	13.3221	8.1521	2.8443
Diff Map	30.2166	29.6940	28.1611	25.6646	22.3125	18.1816	13.4606	8.2916	2.9831
LLE	30.2003	29.6894	28.1652	25.6854	22.3254	18.1924	13.4682	8.2789	2.9805
Subject K									
ICA	30.1220	29.5681	28.0250	25.5203	22.1783	18.0569	13.3136	8.2129	2.9432
Isomap	30.1864	29.6640	28.1538	25.6675	22.2939	18.1749	13.4683	8.2771	2.9618
Diff Map	30.2093	29.7037	28.1519	25.6816	22.3158	18.2034	13.4654	8.2952	2.9904
LLE	30.2080	29.6818	28.1548	25.6716	22.3262	18.1962	13.4695	8.2875	2.9790
Subject S									
ICA	30.2240	29.7156	28.1836	25.6819	22.3365	18.2140	13.4956	8.3269	3.0025
Isomap	30.2044	29.7038	28.1697	25.6823	22.3215	18.2035	13.4576	8.2912	2.9832
Diff Map	30.2066	29.6898	28.1527	25.6871	22.3178	18.1870	13.4652	8.2941	2.9765
LLE	30.1965	29.6953	28.1583	25.6731	22.3160	18.1937	13.4655	8.2990	2.9525
Subject T									
ICA	30.2336	29.7114	28.1868	25.6938	22.3342	18.2210	13.4869	8.3183	3.0027
Isomap	30.2077	29.6922	28.1493	25.6869	22.3167	18.1991	13.4576	8.2959	2.9792
Diff Map	30.2115	29.6900	28.1641	25.6714	22.3120	18.1877	13.4735	8.2751	2.9868
LLE	30.2100	29.6754	28.1444	25.6737	22.3142	18.1942	13.4569	8.2977	2.9799
Subject W									
ICA	30.2307	29.7087	28.1928	25.7006	22.3436	18.2214	13.4755	8.3068	2.9984
Isomap	30.1833	29.6769	28.1525	25.6727	22.3140	18.1835	13.4538	8.2765	2.9460
Diff Map	30.2106	29.6915	28.1508	25.6780	22.3146	18.1972	13.4617	8.2923	2.9748
LLE	30.2044	29.6896	28.1588	25.6591	22.3199	18.1946	13.4617	8.3007	2.9805

Table 2: Time domain comparison using Postle *et al.* dataset. Correlation of power spectra for activation time courses generated for each subject using ICA and the various dimensionality reduction methods: ICA (ICA alone), Isomap (Isomap and ICA), LE (Laplacian eigenmap and ICA), and LLE (Local linear embedding and ICA).

Subject	ICA	Isomap	LE	LLE
H	0.7771	0.6944	0.8600	0.8774
K	0.9412	0.7288	0.8229	0.7897
S	0.8423	0.7319	n/a	0.8719
T	0.8903	0.7657	0.8274	0.8094
W	0.9262	0.7156	0.8268	0.8711

squares, subjects were asked to recreate the sequence from that point on. In the manipulate memory task, subjects were asked to reorder the highlighted sequence of squares from bottom to top, so that the lowest highlighted square should be first in the sequence and the highest should be last. In the guided saccade task, subjects were asked to simply follow another highlighted sequence on the screen. In the free saccade task, subjects were not shown a highlighted sequence, and were asked to simply saccade left and right repeatedly.

In these experiments, we consider a ROI based on the reported areas in each subject. We constrain the ROI to be even smaller. In this experiment, we use the manipulate memory task as the experimental task alone and generate the reference function for each subject.

Time Domain Experiment. We apply the method to time domain signals, as in the left/right task. In this case, dimensionality reduction methods produce signals that do not compare on the time axis. In this case, we compare the correlation of the power spectra from activation time courses to the reference power spectrum. Here we compare the first 50 frequency values, accounting for over 99% of the frequency content in the reference signal. ICA generated components are well correlated across subjects. However, local linear embedding appears to outperform ICA in subjects H and S (see Table 2).

Frequency Domain Experiment. We apply the method to the frequency domain signals using the same comparison method used in the left/right dataset. In this case, dimensionality reduction methods outperform ICA alone for most subjects. For sub-

ject H, Isomap appears to recover sources whose activation better matches the reference function. For subject K, ICA alone appears to outperform the manifold learning methods. For subjects S,T, and W, manifold learning appears to generate better source separation.

5 DISCUSSION

In our method, we motivate manifold learning as a pre-processing step to convolutive source separation by appealing to the need for dimensionality reduction. The idea in using manifold learning to reduce dimensionality is that we can automatically identify the voxels in the ROI that contain the most information about the activation sequence of the area. Furthermore, the frequency space representation of voxels results in much higher dimensionality; therefore, reducing the dimensionality is critical to feasible component analysis. The computational cost of filtering unneeded dimensions at component analysis time is far greater than at manifold learning time.

An additional side effect of manifold learning is that we not only find features representing the activation in an area, but we also space the data along these features so that we implicitly perform whitening of the data. In the normal use of time domain ICA one explicitly performs PCA as a first step in order to whiten the data. In the time domain this decorrelates the data, making the source separation task return better results.

We have shown improvement by using manifold learning as a preprocessing step to complex source separation. One benefit of this method is that the reduced dimensionality representation requires less computation by complex ICA. Furthermore, little prior information is needed to define the ROI. These results suggest that a more tightly integrated approach would lead to better separation performance.

REFERENCES

Anemuller, J., Sejnowski, T., and Makeig, S. (2003). Complex independent component analysis of frequency-domain electroencephalographic data. *Neural Networks*, 16:1311–1323.

Belkin, M. and Niyogi, P. (2003). Laplacian eigenmaps for dimensionality reduction and data representation. *Neural Computation*, 15:1373–1396.

Bingham, E. and Hyvarinen, A. (2000). A fast fixed-point algorithm for independent component analysis of complex valued signals. *International Journal of Neural Systems*, 10(1):1–8.

Coifman, R. R. and Lafon, S. (2006). Diffusion maps. *Applied and Computational Harmonic Analysis*, 21:5–30.

Dogil, G., Ackerman, H., Grodd, W., Haider, H., Kamp, H., Mayer, J., Reicker, A., and Wildgruber, D. (2002). The speaking brain: a tutorial introduction to fmri experiments in the production of speech, prosody, and syntax. *Journal of Neurolinguistics*, 15(1):59–90.

Friston, K. (2003). Experimental design and statistical parametric mapping. In et al., F., editor, *Human brain function*. Academic Press, 2nd edition.

Hurd, M. (2000). Functional neuroimaging motor study.

Josephs, O., Turner, R., and Friston, K. (1997). Event-related fmri. *Human Brain Mapping*, 5(4):243–248.

McKeown, M. J., Makeig, S., Brown, G. G., Jung, T. P., Kindermann, S. S., Bell, A. J., and Sejnowski, T. J. (1998). Analysis of fmri data by blind separation into independent spatial components. *Human Brain Mapping*, 6:160–188.

Pederson, M. S., Larsen, J., Kjerns, U., and Parra, L. C. (2007). *Springer handbook on speech processing and speech communication*, chapter A survey on convolutive blind source separation methods. Springer Press.

Postle, B. R., Berger, J. S., Taich, A. M., and D'Esposito, M. (2000). Activity in human frontal cortex associated with spatial working memory and saccadic behavior. *Journal of Cognitive Neuroscience*, 12 Supp. 2:2–14.

Roweis, S. and Ghahramani, Z. (1999). A unifying review of linear gaussian models. *Neural Computation*, 11:305–345.

Roweis, S. and Saul, L. (2000). Nonlinear dimensionality reduction by locally linear embedding. *Science*, 290(5500):2323–2326.

Shen, X. and Meyer, F. G. (2006). Nonlinear dimension reduction and activation detection for fmri dataset. In IEEE, editor, *Proceedings of 2006 conference on computer vision and pattern recognition workshop*. IEEE.

Tenenbaum, J., de Silva, V., and Langford, J. (2000). A global geometric framework for nonlinear dimensionality reduction. *Science*, 290(5500):2319–2323.